Int. J. Multiphase Flow Vol. 17, No. 2, pp. 191–211, 1991
Printed in Great Britain

0301-9322/91 $3.00 + 0.00
Pergamon Press/Elsevier

DIRECT CONTACT CONDENSATION OF STEAM ON DROPLETS

G. P. CELATA, M. CUMO, F. D'ANNIBALE and G. E. FARELLO
ENEA TERM/ISP-Casaccia, Via Anguillarese 301, Roma, Italia

(Received 23 November 1989; in revised form 12 October 1990)

Abstract—An experiment of direct contact condensation of saturated steam on subcooled water sprays characterized by droplets of uniform size has been carried out with the aim of testing the influence of droplet diameter and velocity on the heat transfer rate, up to a pressure of 0.6 MPa. Liquid sprays with a uniform distribution of droplet diameters (in the range 0.3–2.8 mm) were obtained by means of an *ad hoc* injection system based on the superposition of a high frequency acoustic vibration in the liquid. Continuous measurements of the average droplet temperature along the axis of the spray jet were performed. The condensation efficiency and local heat transfer coefficient were calculated as functions of the main parameters involved (droplet diameter and velocity, thermodynamic condition of the fluids). Comparisons of experimental results with predictions obtained using available models are reported. A method allowing a better data reduction, based on consideration of the turbulence inside the droplet, is proposed.

Key Words: uniform size, droplets, direct contact, condensation, spray, steam-water, experimental data

INTRODUCTION

Direct contact condensation of vapour on dispersed droplets of subcooled liquid has many industrial applications, particularly in the chemical (degassers, mixing-type heat exchangers) and nuclear (emergency core cooling systems) industries. Consequently, numerous studies have been conducted on the subject. Considerable effort has been directed towards the theoretical description of the phenomenon, as reported in the next section.

On the other hand, there is insufficient experimental data for a full understanding of the phenomenon and for clarification of the relative merits of each model in various situations. The available data refer to either sprays characterized by a probability density function of the droplet size distribution, or single droplets having a narrow range of diameters. In the first case, it is only possible to deduce macroscopic information about the heat transfer characteristics of the particular spray employed. In the second case, the greatly reduced ranges of droplet diameter and velocity do not allow full comprehension of the fundamental aspects of the phenomenon.

The aim of the present work was to investigate the influence of droplet diameter and velocity, as well as the thermodynamic conditions of steam and water, on the heat transfer from saturated steam to subcooled water droplets. Sprays characterized by uniform-size liquid droplets were employed, varying the droplet from 0.3 to 2.8 mm, and the droplet velocity from 0.85 to 9.0 m/s. Thus, it was possible to relate heat transfer not to the average droplet diameter of the spray, i.e. to a statistical definition of the heat transfer area, but to the actual diameter of the spray droplets, in an extended range of parameters of interest.

LITERATURE SURVEY

Experiments

A survey of the open literature reveals a lack of data regarding condensation of vapour on liquid droplets. Experiments by Weinberg (1952) refer to a water spray produced with centrifugal nozzles of a commercial type. Ford & Lekic (1973) carried out experiments with single water droplets of 1.51 and 1.76 mm dia and with water sprays produced with commercial full-cone type nozzles (Ford & Lekic 1980). Ohba *et al.* (1982) performed an experiment with a water spray having a mean droplet diameter of about 0.4 mm and a mean droplet velocity of about 40 m/s. Hijikata *et al.*

(1984) conducted an experiment of condensation of vapour on single droplets of 2.0 mm, employing refrigerant R-113 and methanol as working fluids. Isachenko & Solodov (1972) reported experiments with water sprays having average droplet diameter of 0.08–0.25 mm.

Theoretical analyses

Proposed mathematical models may be grouped on the basis of the hypotheses adopted:

(a) Pure conduction in the droplet, without thermal resistance on the steam side (Ford & Lekic 1973, 1980; Pasamehmetoglu & Nelson 1987a, b; Dharma Rao & Sarma 1985). This may be valid for small and slow droplets in the absence of non-condensible gas in the steam phase.
(b) Pure conduction in the droplet with thermal resistance on the steam side. This hypothesis may be valid for condensation of multicomponent vapours on small and slow droplets.
(c) Complete mixing in the droplet (uniform droplet temperature) (Chung & Ayyaswamy 1977), for an environment with either a low supply of steam or a considerable amount of non-condensible gas.
(d) Internal circulation in the droplet (Ohba *et al.* 1982; Huang & Ayyaswamy 1987; Chung & Chang 1984) for big and fast droplets.
(e) Internal mixing in the droplet (Rose & Kintner 1966) due to oscillations of the droplets, for droplets characterized by $Re_S > 200$.

Considering the present experiment, the models of group (a), by Ford & Lekic (1973, 1980) and Pasamehmetoglu & Nelson (1987a, b), group (d), by Ohba *et al.* (1982), and group (e), by Rose & Kintner (1966), are of interest.

Among the empirical correlations proposed in the literature (Weinberg 1952; Isachenko & Solodov 1972; Brown 1951; Carra & Morbidelli 1986), it is worth testing those proposed by Skelland & Wellek (1964) for turbulent oscillating and non-oscillating droplets.

Pure conduction model

This approach is based on the assumption that the process of vapour condensation could be treated as transient heat transfer to a solid sphere with negligible resistance at the interface. The applicable differential equation is

$$\frac{\partial\theta}{\partial t} = \alpha\left(\frac{\partial^2\theta}{\partial r^2} + \frac{2}{r}\frac{\partial\theta}{\partial r}\right), \qquad [1]$$

θ being the non-dimensional temperature, defined as $(T - T_{w0})/(T_s - T_{w0})$, and α, the thermal diffusivity of water. The subscripts w and s denote water and steam, respectively, while 0 refers to the initial conditions.

With the following boundary conditions:

(1) $\theta(r, 0) = 0$, drop initially at a uniform temperature;
(2) $\theta(R, t) = 1$, drop surface at $r = R$ immediately reaches saturation temperature;
(3) $(\partial\theta/\partial r)_{r=0} = 0$, symmetry;

the appropriate temperature distribution, considering (as an approximation necessary for the solution) that the sphere radius remains constant, is given by

$$\theta(r, t) = 1 - \frac{2R}{\pi r}\sum_{n=1}^{\infty}\frac{(-1)^n}{n}\sin\left(n\pi\frac{r}{R}\right)\exp\left(-\alpha\frac{\pi^2 n^2 t}{R^2}\right). \qquad [2]$$

The average non-dimensional temperature of the droplet is given by

$$\theta_m = 1 - \frac{6}{\pi^2}\sum_{n=1}^{\infty}\frac{1}{n^2}\exp\left(-n^2\frac{4\pi^2\alpha t}{D_0^2}\right), \qquad [3]$$

where D_0 is the (initial) droplet diameter.

Ford & Lekic (1973) model

Ford & Lekic (1973) studied the growth of the droplet due to steam condensation, neglecting the thermal resistance on the steam side and considering the droplet as a rigid sphere, i.e. using practically a pure conduction model. Starting from [1], and taking into account the additional boundary condition

$$(T_s - T_{w0})\left(\frac{\partial\theta}{\partial r}\right)_{r=R} = \lambda\rho\frac{dR}{dt},$$

i.e. the heat balance at the interface, where k is the thermal conductivity and λ the latent heat, they obtained an approximate expression of the growth rate law for the droplet:

$$\frac{D}{D_0} = 1 + \psi\left[1 - \exp\left(-\frac{4\pi^2\alpha t}{D_0^2}\right)\right]^{1/2}; \quad \psi = \left[1 + \frac{C_{pd}(T_s - T_{w0})}{\lambda}\right]^{1/3} - 1. \qquad [4]$$

Ford & Lekic (1980) extended the model to the case of a spray of subcooled liquid droplets produced by a commercial full-cone type nozzle.

Pasamehmetoglu & Nelson (1987a, b) model

Pasamehmetoglu & Nelson (1987a, b) proposed an approach similar to that described above, applying it to droplets in a condensing medium under transient conditions of pressure. Under steady conditions, the difference from the Ford & Lekic (1973) model consists of the introduction of: (a) an empirical correction coefficient to take into account the convective contribution inside the droplet; and (b) a limitation of the steam supply towards the droplet surface. The solution of the Fourier equation in this case yields the average non-dimensional droplet temperature, θ_m, as

$$\theta_m = 1 - \frac{6}{\pi^2}\sum_{n=1}^{\infty}\frac{1}{n^2}\exp\left(-n^2C\frac{4\pi^2\alpha t}{D_0^2}\right), \qquad [5]$$

where C is an empirical "convective" factor.

With the same approximation as made by Ford & Lekic (1973), they obtained

$$\theta_m = \left[1 - \exp\left(-C\frac{4\pi^2\alpha t}{D_0^2}\right)\right]^{1/2}. \qquad [6]$$

According to the authors, the effect of the limitation of the steam supply to the surface of the droplet becomes negligible within 1 ms of the exit of the droplet from the nozzle. Therefore, [5] and [6] can be utilized in most practical cases.

Ohba et al. (1982) model

Ohba *et al.* (1982) proposed a model based on the internal circulation in the droplets. They obtained the velocity fields inside the droplet and on the steam side solving the conservation equations with the finite differences method. The assumptions made are:

1. The mass increment of the droplet due to steam condensation is negligibly small; hence the droplet is kept in a spherical shape with a constant diameter.
2. The thermal resistance of the droplet surface with respect to steam condensation is negligibly small and the surface temperature is always kept at the steam temperature.
3. When the droplet is ejected from a nozzle, an axisymmetrical circulating flow is produced inside it. The strength of the circulation is kept constant.
4. The temperature field has no effect on the flow field of the circulation.
5. All the physical properties are kept constant inside the droplet.

Adopting the stream functions obtained by Hadamard (1911) for the internal circulation, and by Hill, in Lamb (1932), for the velocity field outside the droplet, Ohba *et al.* obtained a differential equation to be solved with the finite differences method. For simplicity, we report here the solution

for infinite circulation inside the droplet, i.e. uniform temperature along the streamlines, as proposed by Kronig & Brink (1950):

$$\theta_m = 1 - \frac{3}{8}\sum_{n=1}^{\infty} A_n^2 \exp\left(-16\beta_n \frac{4\alpha t}{D_0^2}\right), \quad [7]$$

where β_n and A_n are, respectively, the eigenvalues and the coefficients to be determined from the eigenfunctions. Their numerical values (limited to two) were obtained as follows:

$$\beta_1 = 1.678; \quad \beta_2 = 9.83; \quad A_1 = 1.32; \quad A_2 = 0.73.$$

Rose & Kintner (1966) model

Rose & Kintner (1966) developed a model for oscillating droplets of organic liquids in water under the basic hypothesis of the breaking of streamlines due to the oscillations, which gives rise to the internal mixing of the droplet. The droplet is considered as constituted by an inner part, having a uniform temperature, and by an external layer, the thickness δ_x of which is a function of time during the oscillation. The conduction in the superficial layer is taken into account considering the equation for plane geometry:

$$\theta = 1 - \exp\left[-\frac{\alpha}{V_d}\int_0^{t_c} \frac{S_d(t)}{\delta_x}\,dt\right]. \quad [8]$$

Assuming an oblate ellipsoidal shape for the drop, the surface area S_d for the drop of volume V_d is given by

$$S_d(t) = 2\pi a^2 + \frac{\pi b^2}{\sqrt{\frac{a^2-b^2}{a^2}}} \ln\left(\frac{1+\sqrt{\frac{a^2-b^2}{a^2}}}{1-\sqrt{\frac{a^2-b^2}{a^2}}}\right), \quad [9]$$

where a and b are the two ellipsoid semiaxes. The first one is estimated assuming the following oscillation law:

$$a = a_0 + a_p|\sin \omega t|, \quad [10]$$

where a_p is the oscillation amplitude and ω is the angular frequency of oscillation, given by the Schroeder & Kintner modification of Lamb's (1932) equation,

$$(2\omega)^2 = \frac{6.44\sigma}{D^{2.775}}\left(\frac{24}{3\rho_L + 2\rho_s}\right), \quad [11]$$

where σ is the surface tension, and the subscript L denotes the liquid. The second semiaxis b is then given by

$$b = \frac{3V_d}{4\pi a^2} \quad [12]$$

which is derived from the assumption of constant drop volume. The thickness of the interfacial resistance zone δ_x is estimated assuming that its volume remains constant during oscillation of the drop:

$$\delta_x = \frac{[a_0^2 b_0 - (a_0 - \delta_{x0})^2(b_0 - \delta_{x0})] - 2ab\delta_{x0} + b\delta_{x0}^2}{a^2 - 2a\delta_{x0} + \delta_{x0}^2}, \quad [13]$$

where a_0, b_0 and δ_{x0} indicate the initial values. This last quantity is evaluated through the two-film theory as follows:

$$\delta_{x0} = \frac{\alpha}{k_d} \quad [14]$$

where k_d is given by the additivity rule. The local mass transfer coefficient in the continuous phase can be estimated from one of the relationships reported above, and the one for the dispersed phase from penetration theory:

$$k_d = \frac{2}{\pi}\left(\frac{D\omega}{2}\right)^{1/2}, \quad [15]$$

where the characteristic time has been taken as equal to the time for one oscillation cycle.

Skelland & Wellek (1964) empirical relationships

For droplet Reynolds numbers, Re_s, exceeding about 200, the droplet may oscillate between an oblate (or spherical) and a more oblate shape. Such oscillations lead to a stretch of the interfacial surface and to significant internal mixing, which greatly enhances the rate of mass transfer. Several models are proposed in the literature and reviewed in Carra & Morbidelli (1986). Such models are usually complicated but may be approximated by empirical *ad hoc* expressions.

Considering the link between θ and the average droplet Sherwood number, Sh_d,

$$\theta = 1 - \exp(-\tfrac{3}{2}Sh_d\tau), \quad [16]$$

where τ is the non-dimensional time, $\tau = 4\alpha t/D_0^2$, Skelland & Wellek (1964) proposed

$$Sh_d = 0.32\tau^{-0.141}Re_s^{0.683}M^{-0.1}, \quad [17]$$

where M is the Morton number. Relationship [17] is valid for oscillating droplets in the range $330 < Sh_d < 3600$ and $400 < Re_s < 3100$. The oscillating droplet regime may be considered for big and fast droplets.

For non-oscillating turbulent droplets the same authors proposed

$$Sh_d = 31.4\tau^{-0.338}Sc_d^{-0.125}We^{0.371}, \quad [18]$$

where Sc_d is the droplet Schmidt number and We the Weber number.

THE EXPERIMENTAL APPARATUS

The experimental loop

A diagram of the experimental setup, already employed for the experiments of Celata *et al.* (1989a), is shown schematically in figure 1. The apparatus includes the test section, the water storage tank, an electric heater for the water (10 kW), an electric boiler for saturated steam production (15 kW) and an electric heater for steam superheating. The loop characteristics are as follows:

Pressure	up to 1.0 MPa
Water mass flow rate	up to 120 kg/h
Steam mass flow rate	up to 20 kg/h
Inlet saturated steam temperature	up to 160°C
Inlet water temperature	up to 80°C
Inlet superheated steam temperature	up to 200°C

The test section (figure 2) consists of a cylindrical vessel flanged at the bottom. Steam, generated using degassed water, is supplied from the top of the vessel. Steam is continuously purged through a bleeding line to prevent the accumulation of non-condensible gas in the test chamber. Pressurized water (degassed before filling the vessel, and then pressurized with nitrogen to have a strictly constant water mass flow rate) is supplied by means of a multihole nozzle into the test chamber in the form of a spray jet. The amount of non-condensibles is not known, but we have tried to obtain the maximum value considering the nitrogen dissolved in the water to be completely released. This value is about 50–70 ppm; incidentally, the real fraction of gas released by the droplet (and then the concentration) should be much lower even though not directly evaluable. The spray jet is characterized by a uniform distribution of the droplet diameters obtained by means of an *ad hoc* injection system based on the superposition of sine-shaped axisymmetrical disturbances, i.e. acoustic vibrations, on the liquid jet.

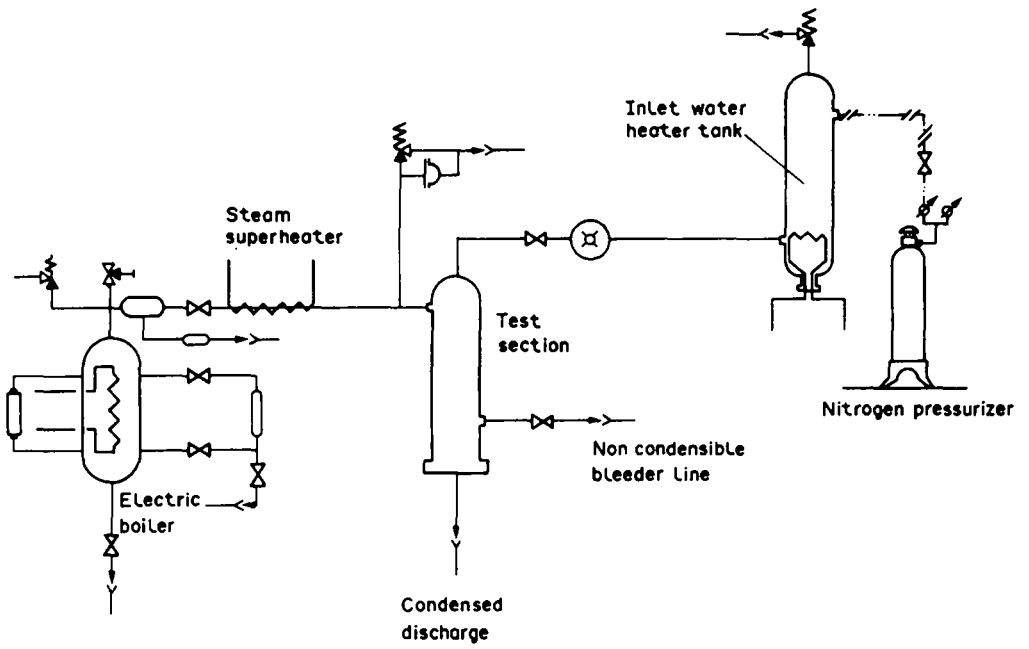

Figure 1. Schematic of the experimental loop.

The average temperature of the droplets is obtained by catching them with a very small catcher of Teflon, which can continuously move along the spray jet axial position. The droplets are collected in a cavity always filled with water (continuously drained from the bottom during the test), whose temperature is measured using two 0.25 mm K-type thermocouples inserted at two different levels. Because of temperature oscillations during the test, data acquisition is accomplished using a graphic recorder.

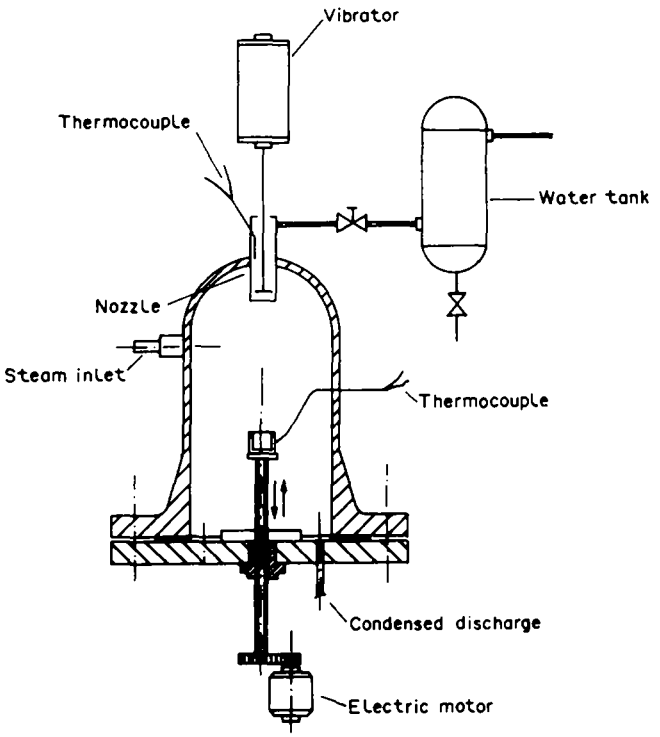

Figure 2. Schematic of the test section.

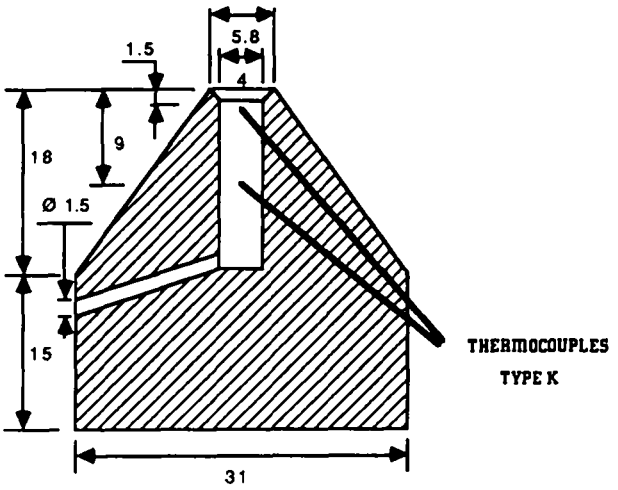

Figure 3. Schematic of the droplet catcher (dimensions in mm).

The catcher, sketched in figure 3, was designed to prevent spoiling of the measurement because of (a) condensation of the steam trapped below the water and (b) heat transfer by conduction through the Teflon walls. Steam trapping has been limited by decreasing the diameter of the catcher cavity: decreasing the impact surface, the penetration of the droplet is reduced, and, consequently, so is steam trapping. In fact, in this way, because of gravity and wall friction, the droplet slows down much more quickly inside the water and therefore the volume of the steam trapped is reduced. Regarding point (b) the shape of the catcher enables the non-collected droplets to cool down the external conical surface. Measurement of the temperature inside the Teflon wall thickness revealed a practically negligible thermal gradient around the measurement cavity.

Droplet breakup and shattering which could spoil the measurement because of the increase in the surface heat transfer in the proximity of the catcher surface, can be neglected considering: (1) the extremely small residence time of possible shattered droplets before collection; and (2) the small temperature difference between the steam and the droplets (shattered droplets are essentially generated from the outer layer of the impacting droplet, the temperature of which is close to the saturation value).

Concerning the accuracy achievable with this method, it can be said that: (i) stochastic errors are very limited in view of the good reproducibility of the tests; and (ii) the systematic error due to the method may be considered limited by the design criteria and confirmed by the small difference in the two temperatures given by the two thermocouples inside the catcher. Anyway, the systematic error may be almost cancelled by proper data reduction, as discussed in the section Experimental Results and Data Analysis.

The inlet water temperature is measured with a thermocouple just upstream of the multihole nozzle, and the water mass flow rate by means of turbine flow meters.

The water injection system

As is well-known, a liquid forced through a fine orifice gives rise to a free jet, which is unstable due to surface tension forces (capillarity forces) and disintegrates into droplets (Weber theory). Applying small periodical deformations to the jet surface, the jet disintegrates into droplets with the same mechanism of varicose break-up, but with the frequency of the vibration. As a consequence, droplets of a constant diameter are generated (König & Frohn 1983; Wiegand 1970). In the present case, acoustic vibrations have been superimposed on the liquid just upstream of the multihole nozzle by means of a small brass piston attached to a mechanical vibrator and placed inside the tube which ends with the nozzle itself, as shown in figure 4. If the velocity of the water through the hole is u and the frequency of the vibrator f, the wavelength, s is given by

$$s = \frac{u}{f}. \qquad [19]$$

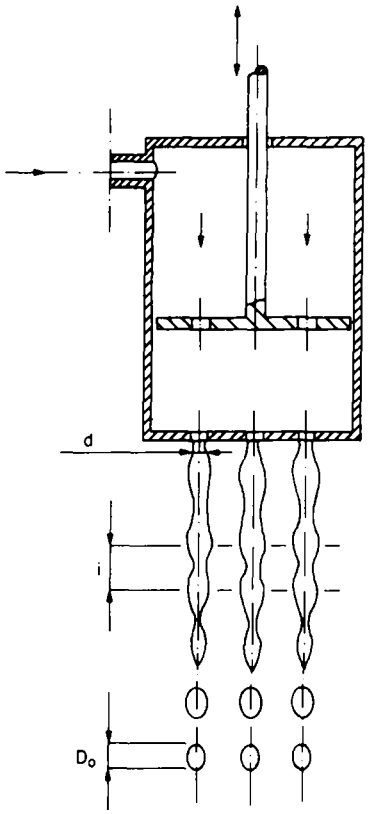

Figure 4. Schematic of the water injection system.

Then the droplet diameter, D, will be given by

$$D = \left(\frac{3u}{2f}d^2\right)^{1/3}, \qquad [20]$$

where d is the diameter of the liquid jet, i.e. of the nozzle holes.

According to Lord Rayleigh (1878), for the case of a non-viscous liquid jet (e.g. water) disintegrating without the influence of air, the best frequency, f_{opt}, of the vibration is given in a first approximation by

$$f_{opt} = \frac{u}{\pi d\sqrt{2}} \approx 0.225\frac{u}{d}. \qquad [21]$$

Then, at the formation of a spherical drop form, the diameter is given by

$$D \approx 1.89d \quad (\text{at } f = f_{opt}). \qquad [22]$$

In a more recent experimental investigation (Schneider & Hendricks 1964) it has been reported that for a constant jet diameter, d, the droplet size can be varied without difficulty when the frequency f is varied within the empirical limit values f_{min} and f_{max}:

$$f_{min} = 0.143\frac{u}{d} < f < 0.286\frac{u}{d} = f_{max}. \qquad [23]$$

The values of f_{opt}, f_{min} and f_{max} adopted in this work were determined experimentally by means of visual observations with a strobo-light, pictures and digital image processing analysis. They are in good agreement with the values calculated by Lord Rayleigh (1878) for f_{opt} and by Schneider & Hendricks (1964) for f_{min} and f_{max} (all data are within $\pm 20\%$). The comparison between experimental and calculated values of f_{opt} is plotted in figure 5.

Six different types of multihole nozzles were employed, as detailed in Table 1. Figure 6(a) is a typical picture of droplets obtained using this system, for $d = 0.4$ mm and $u_d = 1.7$ m/s; the average

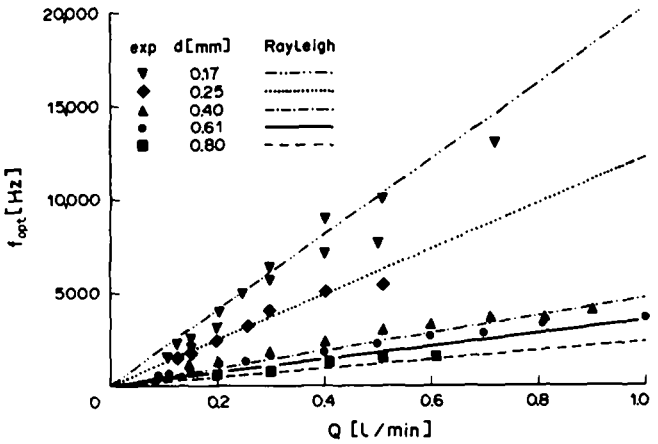

Figure 5. Comparison between experimental and calculated values of f_{opt}.

Table 1. Characteristics of multihole nozzles

d (mm)	No. of holes	Total area (mm^2)
0.17	48	1.09
0.25	25	1.23
0.40	16	2.01
0.61	6	1.75
0.80	4	2.01
1.50	1	1.77

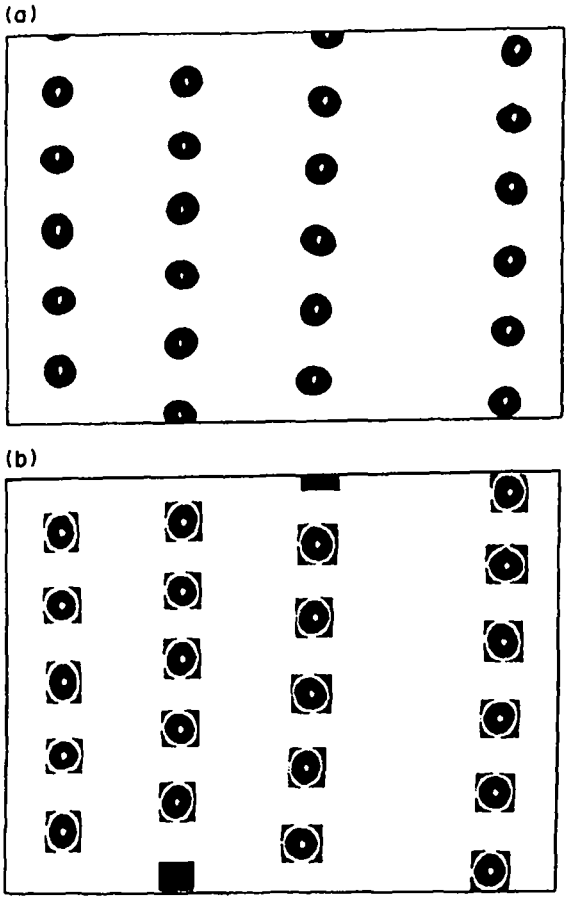

Figure 6. (a) Typical pictures of droplets obtained with the present water injection system—$d = 0.4$ mm, $u_d = 1.7$ m/s, $D = 0.72$ mm. (b) Typical picture taken during the digital image processing analysis.

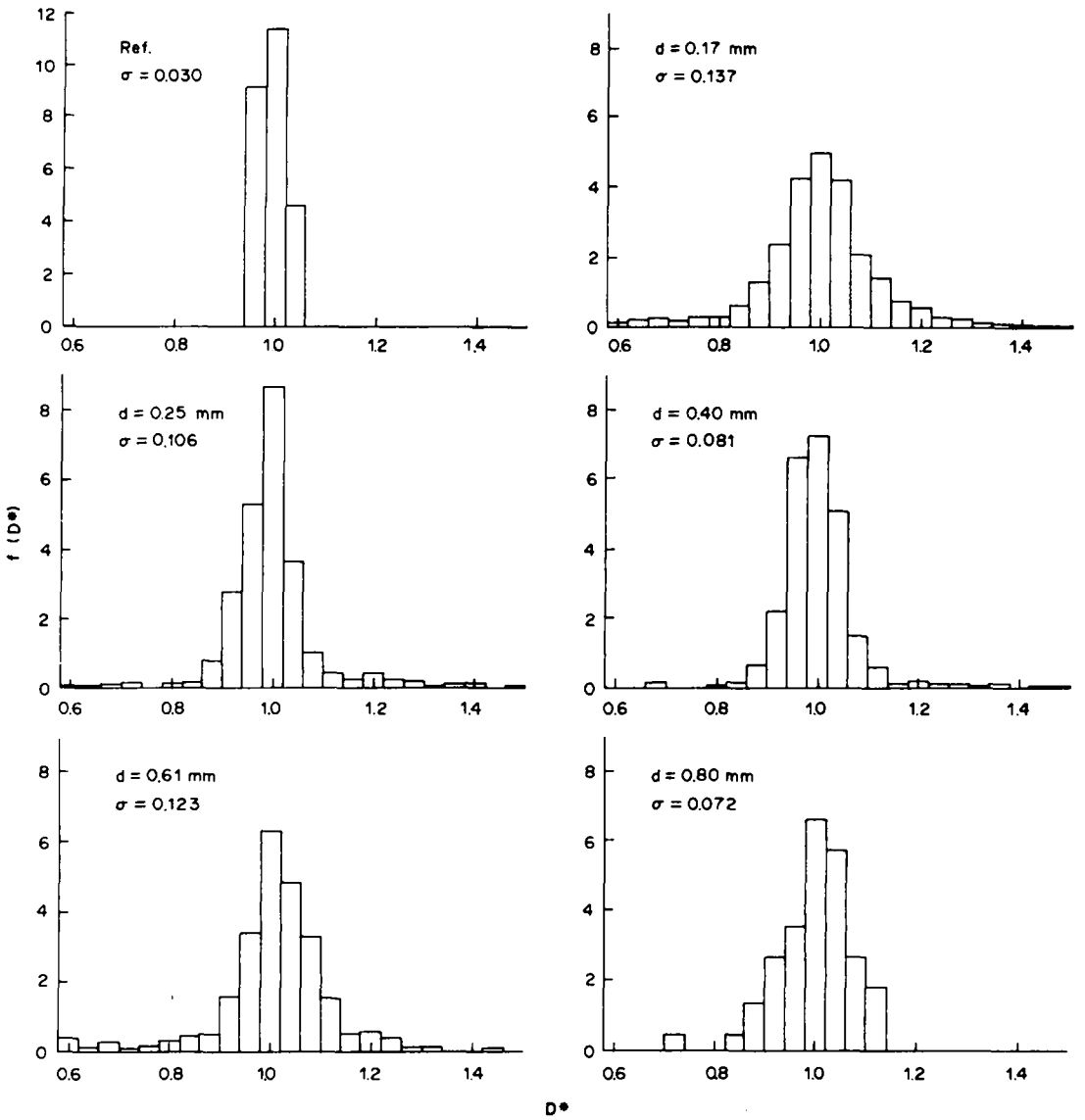

Figure 7. Probability density function of droplet diameter for the multihole nozzles used.

droplet diameter is 0.72 mm. Figure 6(b) is a typical picture taken during the digital image processing analysis of the same droplets. The boxes surrounding the droplets are introduced to enhance the brightness of the droplet edge in the digital processing, i.e. to improve the definition of the system. In figure 7 the probability density function of $D^* = D_{exp}/D_{cal}$, $f(D^*)$, is plotted vs D^* for the reference image (brass disks of different and known diameters, on which the system was calibrated) and for the five multihole nozzles.

EXPERIMENTAL RESULTS AND DATA ANALYSIS

The test matrix

The range of variation of the parameters in the experimental program was as follows:

Multihole nozzle diameter, d [mm]	0.17, 0.25, 0.40, 0.61, 0.80, 1.50
Mass flow rate, Γ [g/s]	from 1.7 to 15.0
Steam temperature, T_s [°C]	110, 130, 150
Water nominal temperature, $T_{w,nom}$ [°C]	30, 60
Droplet velocity, u_d [m/s]	from 0.85 to 9.0

The droplet average temperature is measured over a length of 150 mm from the nozzle exit; generally, about 7–10 measurements of the jet temperature are carried out.

Basic definitions

We define the average droplet non-dimensional temperature (sometimes called the condensation efficiency) as

$$\theta = \frac{T_d - T_{w0}}{T_s - T_{w0}}, \qquad [24]$$

where T_d is the average droplet temperature and T_s is the saturated steam temperature; T_{w0} is the droplet reference temperature (i.e. the initial temperature of the droplet), measured at a distance of 5 mm from the nozzle exit. This is to eliminate any systematic error in the measured droplet temperature, due to enhanced condensation during collection of droplets (droplet breakup and shattering).

Such errors have been reduced further by optimizing the droplet catcher and calibrating the measurement device with a microthermocouple. In any event, such a systematic error, if still present, can be cancelled to some extent by calculating θ between two locations (let us say 1 and 2). Then the non-dimensional temperature becomes

$$\theta = \frac{T_2 - T_1}{T_s - T_1}, \qquad [25]$$

where T_1 and T_2 are the actual temperatures at locations 1 and 2. Let, however, the measured temperatures be T_{2r} and T_{1r}, then the measured non-dimensional temperature is

$$\theta_r = \frac{T_{2r} - T_{1r}}{T_s - T_{1r}}. \qquad [26]$$

Now we need to compare θ_r with θ. Assuming that the error in measuring T_r is equal to $E(T_s - T_r)$, with E a constant, we find

$$\theta = \frac{(\theta_r + E\theta_r)(T_s - T_{1r})}{(1 + E)(T_s - T_{1r})} = \theta_r. \qquad [27]$$

Equation [27] indicates that according to the hypothesis made (proportionality between the error and $T_s - T_r$), this type of systematic error can be eliminated if θ is calculated using two measurements of T_d at two different jet axial positions (one of which is the reference one). Even though this correction may not be perfect, there is undoubtedly a compensatory effect in calculating the non-dimensional temperature in this manner, yielding a value as close as possible to the actual one.

We call z the distance between the point at which the droplet temperature is measured and the point at which the droplet reference temperature is obtained. The local heat transfer coefficient at a given position z, h_{loc}, can be derived from the thermal balance for the droplet travelling at the velocity u_d (local velocity):

$$m_d C_{pd} u_d \frac{dT_d}{dz} = h_{loc} S_d (T_s - T_d), \qquad [28]$$

where T_d is the local value of the average droplet temperature, m_d, C_{pd} and S_d are the mass, the specific heat and the surface of the droplet, respectively.

The local heat transfer coefficient is given by

$$h_{loc} = \frac{D\rho_d u_d C_{pd}}{6(T_s - T_d)} \frac{dT_d}{dz}, \qquad [29]$$

where ρ_d is the droplet density.

Experimental uncertainty and repeatability

The non-dimensional droplet temperature, θ, is deduced from the measured temperatures. According to an error propagation analysis, errors in such measurements, as well as in the

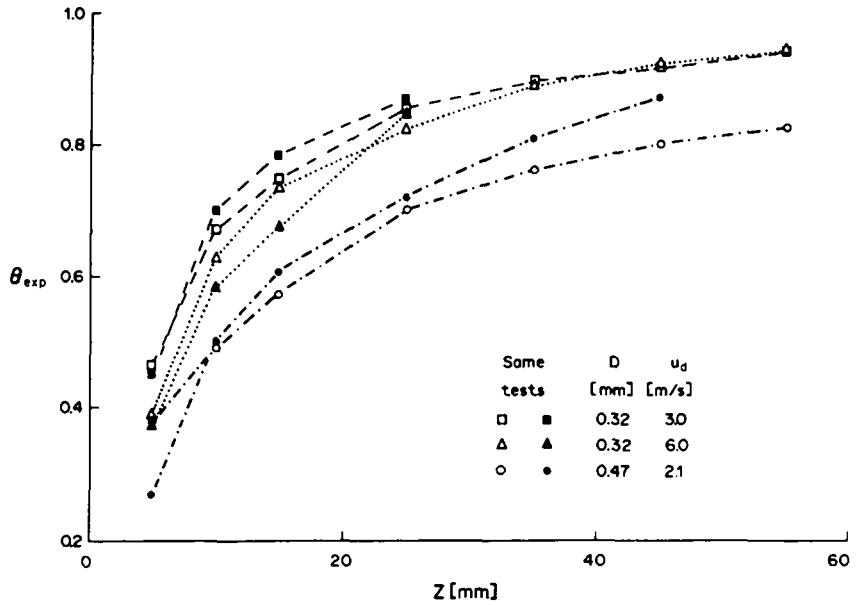

Figure 8. Non-dimensional droplet temperature vs spray jet axial position for several repeated runs.

positioning of the travelling droplet catcher, give rise to the experimental uncertainty in θ. Considering a systematic error of the thermocouples equal to 0.5°C, an error for each temperature measurement due to the uncertainty in the readings of the graphic recorder (steam temperature, max $\pm$ 1.0°C; local droplet temperature, T_d, max $\pm$ 0.5°C; and reference droplet temperature, T_{w0}, max $\pm$ 1.0°C) and an error due to the positioning of the travelling droplet catcher (max $\pm$ 0.5 mm), the experimental uncertainty on θ ranges from 5 to 20% for most of the experimental data (80% of data on a total of 1113 tests). The error in the positioning of the droplet catcher is predominant for low values of z coupled with high values of T_s and low values of T_{w0}. On the other hand, high values of T_{w0} and low values of T_s represent the worst condition apart from the positioning error. It was also observed, in general, that the maximum uncertainty in the experiments was for measurements at small values of z.

A representation of the experimental repeatability is given in figure 8, where θ is plotted vs z, for several repeated runs (u_d is the initial velocity). In the presentation of the experimental results given in the next section error bars have been plotted whenever the clarity of the figures was not compromised.

Experimental data

The complete data set of about 1113 points is reported by Celata *et al.* (1989c). A graphic representation of the data is shown in figures 9 and 10, where the non-dimensional droplet temperature is plotted vs the droplet diameter, D, and the droplet velocity, u_d, respectively. Figure 9 shows two different graphs, grouped according to u_d, at two different values of z. The non-dimensional droplet temperature, for the same z and u_d, turns out to be a strong decreasing function of the droplet diameter, especially at small values of D. This is due to the fact that an increase in the droplet diameter will give rise to a bigger increase in the droplet volume with respect to the droplet heat transfer surface. Thus, the thermal balance for the droplet shows that an increase in the droplet diameter causes a reduction in the droplet temperature, other conditions being equal. Of course this effect tends to disappear for large diameters. It is therefore evident how a spray characterized by a probability density function of droplet diameter may only give macroscopic information about the behaviour of the spray itself, without clarifying the fundamental aspects of the phenomenon.

The influence of the droplet velocity, u_d, on θ is more evident in figure 10, where θ, together with error bars deduced from the error analysis, is plotted vs u_d, for different values of z, with the droplet diameter as a parameter. The behaviour of θ as a function of u_d looks quite complicated. Starting from low values of u_d, θ is first a decreasing function of u_d, then tends to increase as u_d increases

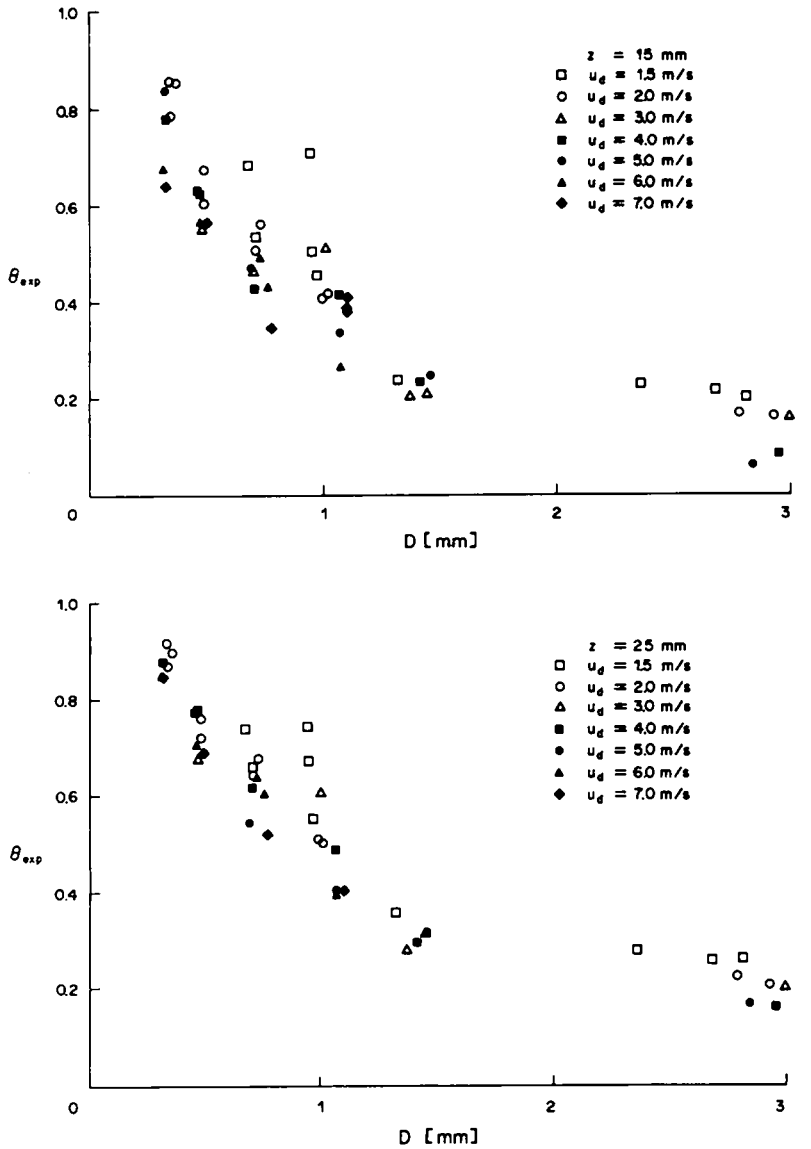

Figure 9. Non-dimensional droplet temperature vs droplet velocity for different droplet diameters; $z = 15$ and $z = 25$ mm.

and, finally, shows a decreasing or almost constant trend for a further increase in u_d. Analogously, figure 11, where θ is plotted vs u_d for some tests with different values of water and steam temperatures, shows the same behaviour together with the observation of a negligible influence of steam and water temperatures. This behaviour has been observed previously in experiments of direct contact condensation of steam either on subcooled water jets (Celata *et al.* 1989a) or on stratified flowing water (Celata *et al.* 1987, 1989b). A qualitative interpretation of this trend may be attempted considering that, apart from internal mixing due to droplet oscillations induced by external (nozzle) and internal agents (surface tension), there is a region where an increase in the droplet velocity causes an enhancement of the internal mixing. This effect, superimposed on the general decreasing trend of the droplet temperature due to the thermal balance may induce a local increase in T_d in terms of droplet velocity.

A typical representation of θ as a function of z is plotted in figure 12, for different droplet diameters and a fixed value of the droplet velocity. The regular trend of θ as a function of z enables a good evaluation of h_{loc} according to [29]. An example regarding the evaluation of h_{loc}, [29], is plotted in figures 13(a, b), where h_{loc} is reported for different droplet diameters: (a) vs the droplet velocity, u_d, at a given z; and (b) vs the distance from the exit, z, for a given u_d. As expected, in

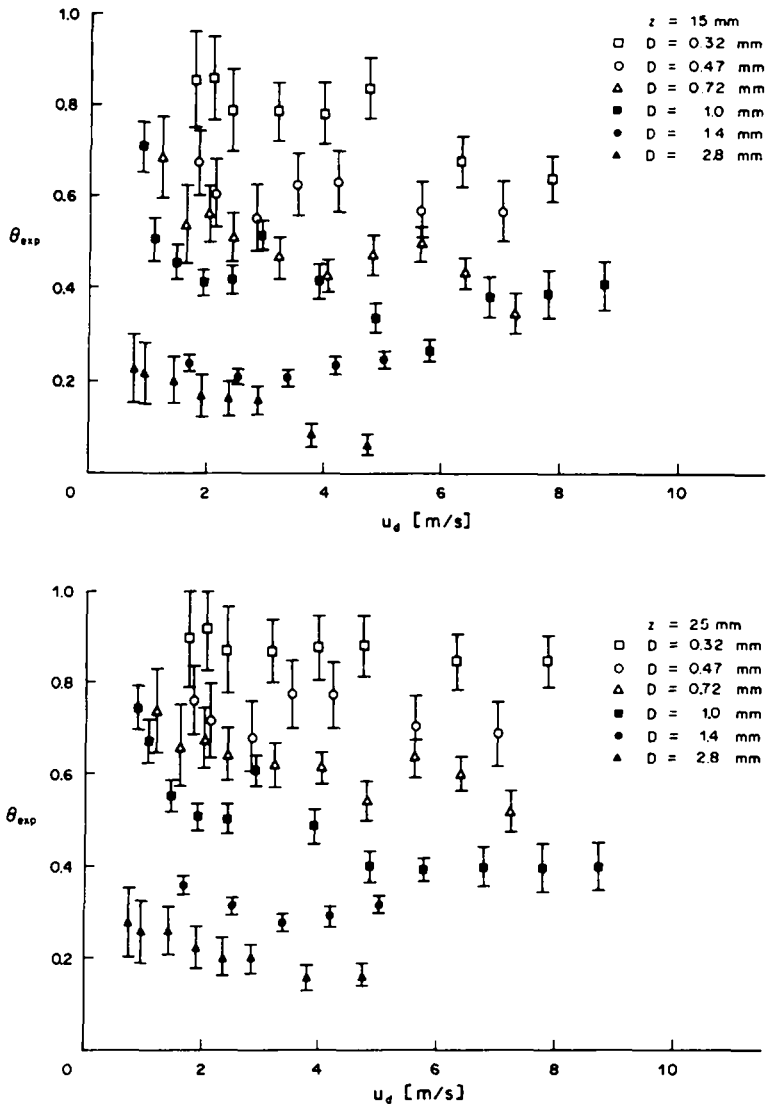

Figure 10. Non-dimensional droplet temperature vs droplet diameter for different droplet velocities; $z = 15$ and $z = 25$ mm.

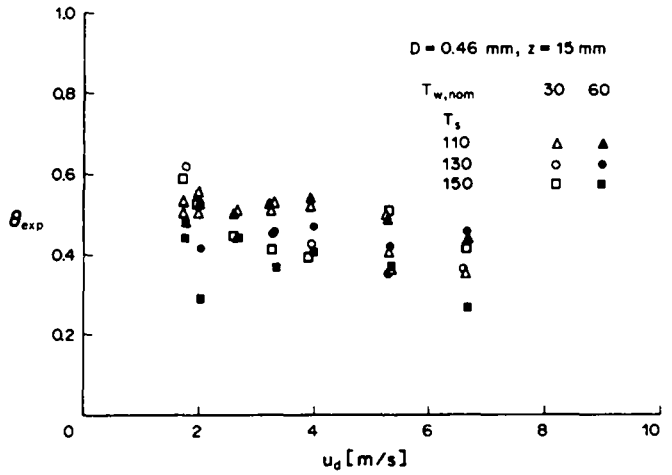

Figure 11. Non-dimensional droplet temperature vs droplet velocity for different values of steam and inlet water temperatures; $D = 0.46$ and $z = 15$ mm.

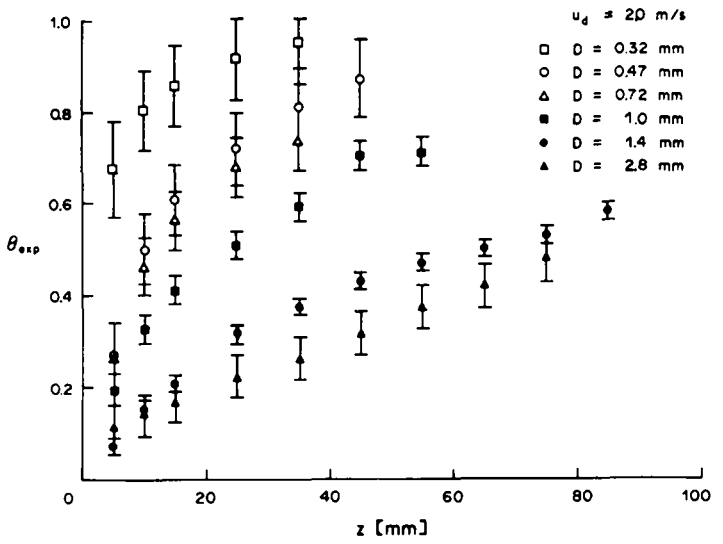

Figure 12. Typical non-dimensional droplet temperature vs spray jet axial position for different droplet diameters and $u_d = 2.0$ m/s.

the investigated range, h_{loc} is a continuous increasing function of the droplet velocity ranging from about 20 kW/m^{2}K at 1 m/s, to about 100 kW/m^{2}K at 8 m/s [figure 13(a)]. At the position $z = 15$ mm, i.e. after the entrance region, the influence of the droplet diameter is quite negligible. For a fixed value of u_d [figure 13(b)], h_{loc} is a decreasing function of z (the derivative dT_d/dz quickly decreases with z) tending to a constant value as z increases. For $z < 15$ mm, the entrance effect gives rise to a consistent spread of the data.

The behaviour of droplets with very large diameters, $D = 2.8$ mm, looks quite different. It may be explained by considering that in this case (figure 12), because of the higher thermal capacity of the droplet in comparison with smaller diameters, the θ vs z trend is always increasing in the investigated range. Practically, the $D = 2.8$ mm droplets belong to a different region of heat transfer and a different behaviour of h_{loc} can be expected.

Data analysis

Models based only on the hypotheses of either pure conduction in the droplet, such as those of Ford & Lekic (1973) and Pasamehmetoglu & Nelson (1987a, b) or internal circulation in the droplet, such as Ohba *et al.* (1982), are not able to explain completely the high values of θ obtained in the experiments. Denoting the Peclet number modified by inclusion of the viscosity ratio, μ,

$$\mathrm{Pe}' = \frac{Du_d}{\alpha}\frac{\mu_s}{(\mu_d + \mu_s)}, \qquad [30]$$

the condition of pure conduction is expressed by $\mathrm{Pe}' = 0$, and the average droplet temperature is obtained by the solution of the Fourier equation

$$\theta_m = 1 - \frac{6}{\pi^2}\sum_{n=1}^{\infty}\frac{1}{n^2}\exp\left(-n^2\frac{4\pi^2\alpha t}{D_0^2}\right). \qquad [31]$$

The condition of infinite circulation (laminar regime) inside the droplet is given by $\mathrm{Pe}' = \infty$, and the solution of the Fourier equation is given by [7].

Experimental data are reported in figure 14 for all the values of D, together with predictions obtained with the pure conduction model ($\mathrm{Pe}' = 0$), the infinite circulation model ($\mathrm{Pe}' = \infty$), and the Rose & Kintner (1966) (oscillating regime) model, where θ is plotted vs the non-dimensional parameter τ, given by

$$\tau = \frac{4\alpha t}{D_0^2}. \qquad [32]$$

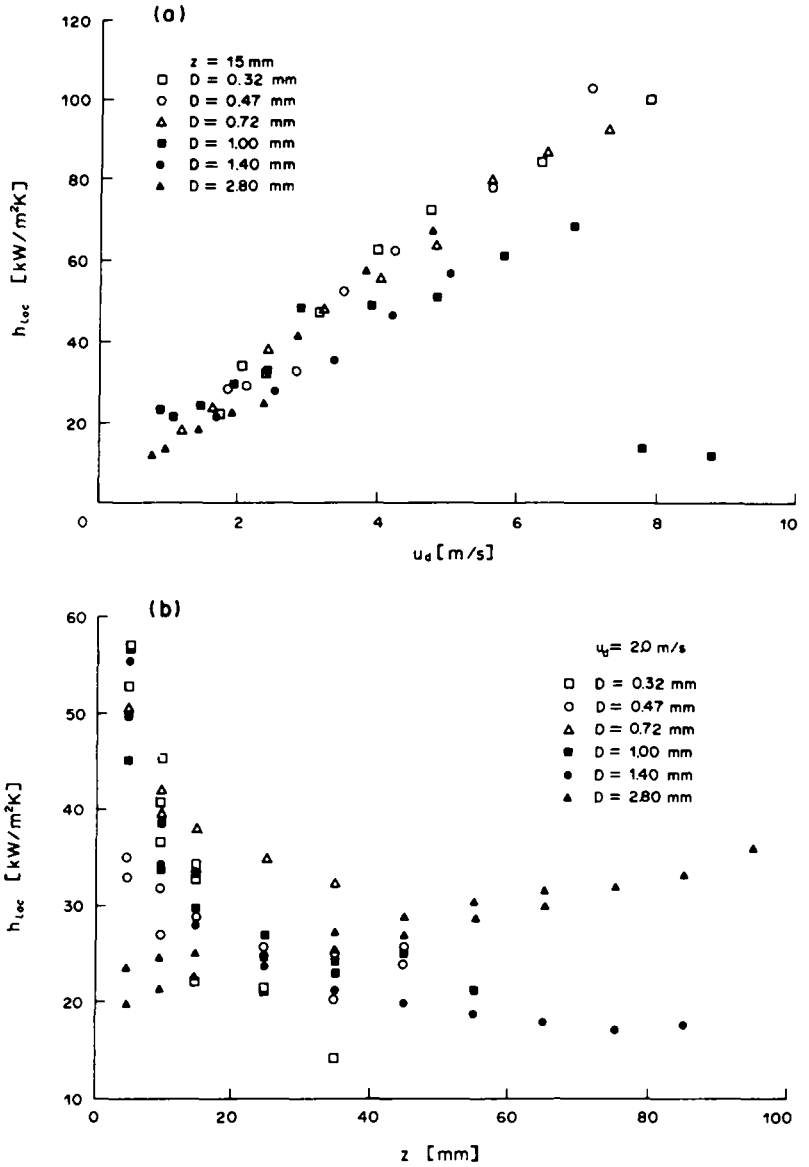

Figure 13. Typical trends of the local heat transfer coefficient vs (a) droplet velocity, $z = 15$ mm, and (b) spray jet axial position; $u_d = 2.0$ m/s; both for different droplet diameters.

The pure conduction model is clearly inadequate for predicting the data. The infinite circulation model instead, is able to give a rough prediction of the data. It underestimates, however, experimental data for $\tau < 0.04$ and very high values of Pe′ (where the model should be applicable) and gives a fairly good agreement for $\tau > 0.04$ and low values of Pe′ (where the model should not be applicable). This behaviour reveals the inadequacy of the assumption of laminar internal circulation inside the droplet (even though for an extreme case of application) in predicting the high condensation efficiency experimentally observed.

In the present experiment, the droplet Reynolds number, Re_s, ranges from 150 to 2000. As reported by Carra & Morbidelli (1986), these values are typical of the oscillating droplet regime described above. The oscillations could give rise to an internal mixing that may be seen as a turbulent contribution to the heat transfer inside the droplet, in addition to the conduction and the transport due to the internal circulation contributions.

The Rose & Kintner (1966) model generally underestimates the experimental values of θ. The main reason is due to the approximation of the external layer by a plane wall. This leads to a considerable underestimation of θ for small values of τ, larger than that of the pure conduction model. Increasing τ, the prediction gets closer to the experimental data.

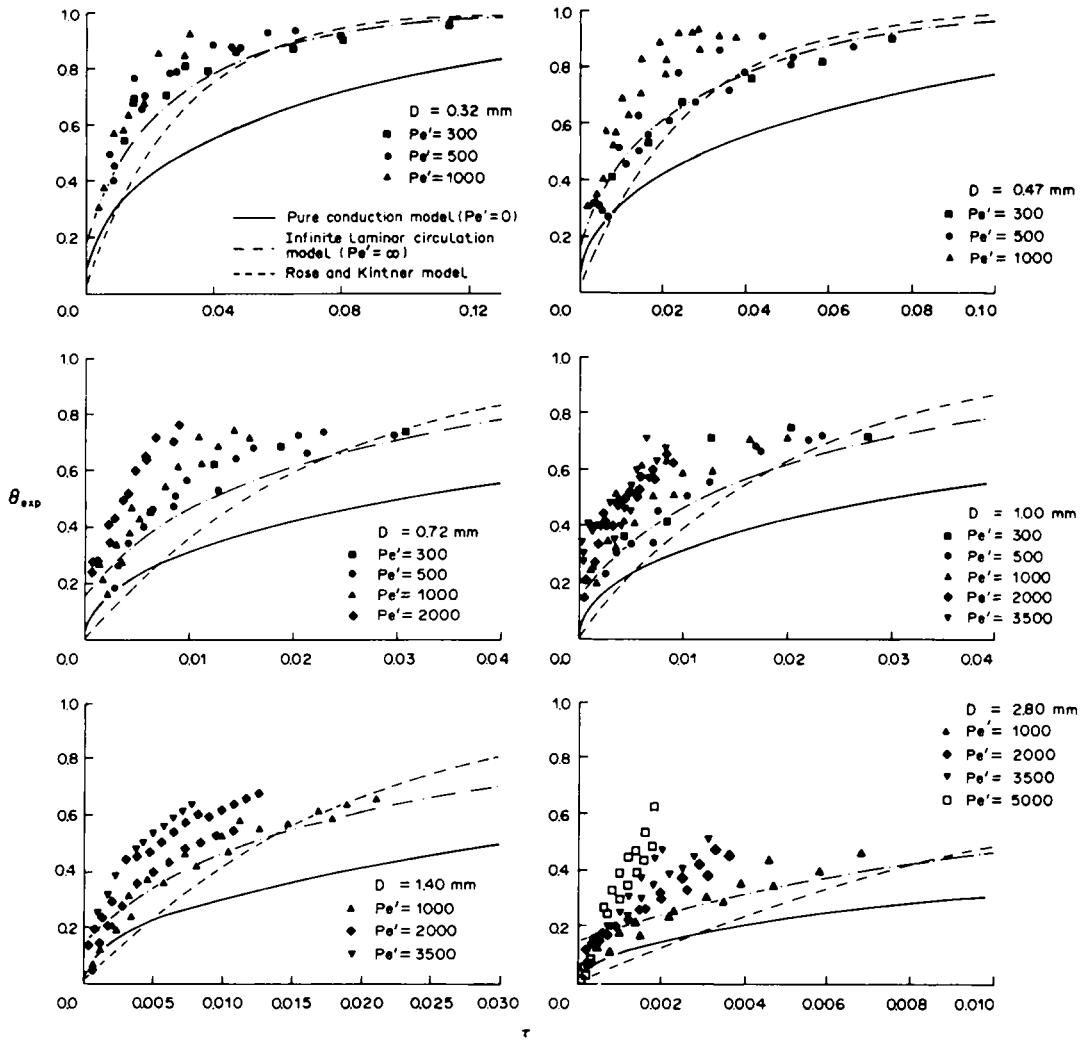

Figure 14. Non-dimensional droplet temperature vs non-dimensional time for different modified Peclet numbers and droplet diameters: experimental results and predictions obtained using the pure conduction model (Pe′ = 0), the infinite circulation model (Pe′ = ∞), and the Rose & Kintner (1966) model.

The empirical relationships proposed by Skelland & Wellek (1964) either for oscillating droplets—[17]—or for non-oscillating turbulent droplets—[18]—have been tested against the experimental data, providing a prediction which does not seem to be consistent. A graphic representation of these predictions will be given below. It is worth reiterating that [17] and [18] were recommended for liquid droplets in a stationary continuous liquid phase, and for systems with low interfacial tensions (between 2.5×10^{-3} and 5.8×10^{-3} N/m).

The inadequacy of the available models and correlations based either on the pure conduction assumption, laminar circulation inside the droplet or approximate accounting for droplet oscillations, in predicting the experimental data, would indicate that the present experimental data lie in the region of the oscillating droplets. One should also consider that:

(a) Photographic observations show droplet oscillations [figures 6(a, b) show droplets whose shape is not spherical].

(b) Hijikata *et al.* (1984), performing an experiment on oscillating droplets using a high-speed camera, claim that the droplet generated by ejection from a nozzle is oscillating by surface tension after leaving the tip of the nozzle. It must be considered that, in our case, the residence time of the droplet in the test chamber is very limited (10–100 ms) to allow a complete action of the damping forces of the surface tension.

(c) According to what was reported by Carra & Morbidelli (1986) for the droplet Reynolds numbers exceeding about 200, the droplet may oscillate between an oblate (or spherical) and a more oblate shape. Such oscillations lead to stretching of the interfacial surface and to a significant internal mixing which greatly enhances the rate of mass transfer. In our experiment the droplet Reynolds number ranged between 150 and 2000, providing the conditions for droplet oscillations, as stated above.

Under these premises, the only way would seem to attempt to define, at least empirically, the turbulent contribution inside the droplet and account for it in the solution of the Fourier equation. Starting from the hypothesis of pure conduction in the droplet, the Fourier equation yields the solution given by [31]. As already proposed by Celata *et al.* (1987, 1989a, b), and as suggested by Pasamehmetoglu & Nelson (1987a), it would be possible to take into account effects of both internal circulation and mixing by means of an empirical convective factor, C, so that [31] becomes [5]. In Celata *et al.* (1987, 1989a, b) it was demonstrated that, as the turbulent contribution can be seen as a macroscopic increase in the thermal conductivity of the liquid, the convective (or turbulent) factor can be expressed as a function of the Reynolds and Prandtl numbers, or, similarly, as proposed by Carra & Morbidelli (1986), as a function of the modified Peclet number:

$$C = a(Pe')^b. \qquad [33]$$

The values of the constants a and b are to be determined empirically on the basis of experimental data. From a best-fit procedure we obtained

$$a = 0.153; \quad b = 0.454$$

A global comparison of experimental data and predictions is reported in figure 15, where the ratio between the calculated and the experimental values of θ is plotted vs τ. Most of the data lie within a $\pm 20\%$ band, even though bigger errors are concentrated in the region of

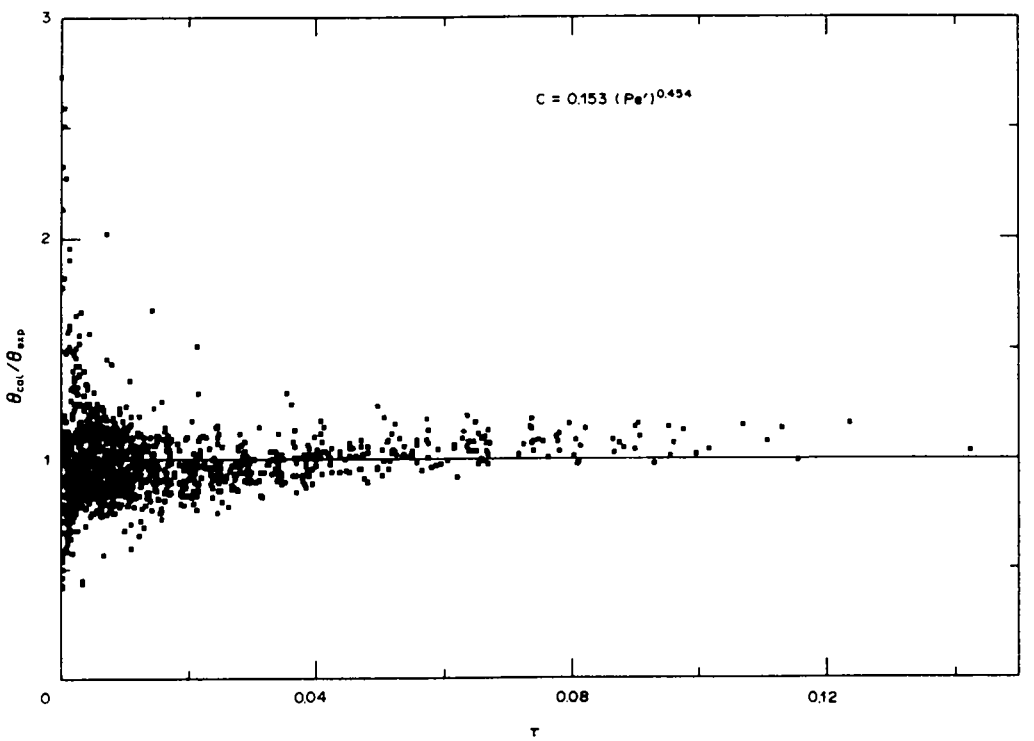

Figure 15. Comparison between experimental values of θ and predictions obtained using [5] and [31] vs non-dimensional time.

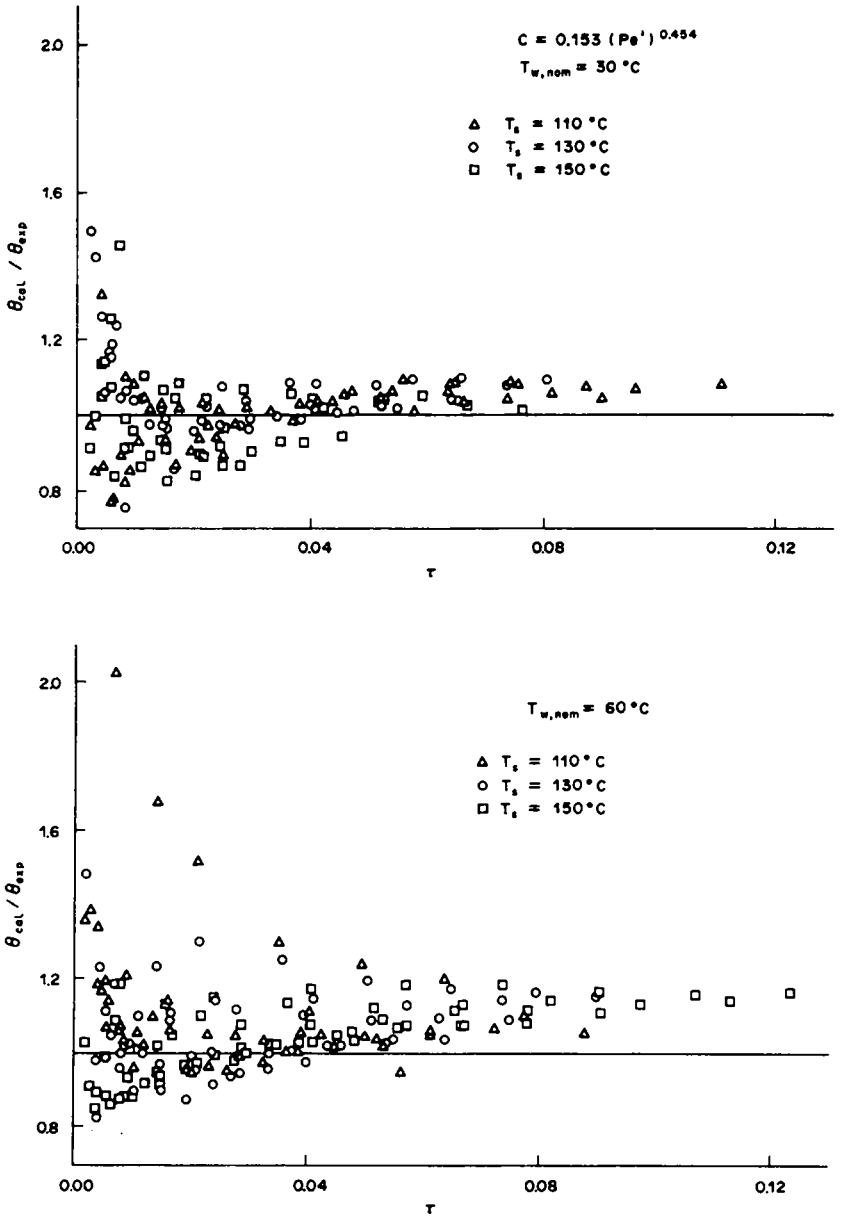

Figure 16. Comparison between experimental values of θ and predictions obtained using [5] and [31] for the different steam and water temperatures investigated.

low values of τ. A similar representation is given in figure 16, where the predictions are grouped by steam temperature, for two different inlet water temperatures. An overall comparison of the predictions obtained with the different models and correlations tested, including the proposed one, is given in figure 17, where dn/dx represents the probability density function of the predictions and is plotted vs the ratio $\theta_{cal}/\theta_{exp}$. Very good agreement is shown by the proposed correlation for the empirical convective factor, C, and a rough prediction is given by the infinite circulation model, as stated before. Other predictions are not consistent with the experimental data.

CONCLUDING REMARKS

An experiment of direct contact condensation of steam on water sprays characterized by uniform-size droplets was conducted with the droplet diameter ranging from 0.3 to 2.8 mm and droplet velocity from 0.85 to 9.0 m/s, with pressures up to 0.6 MPa.

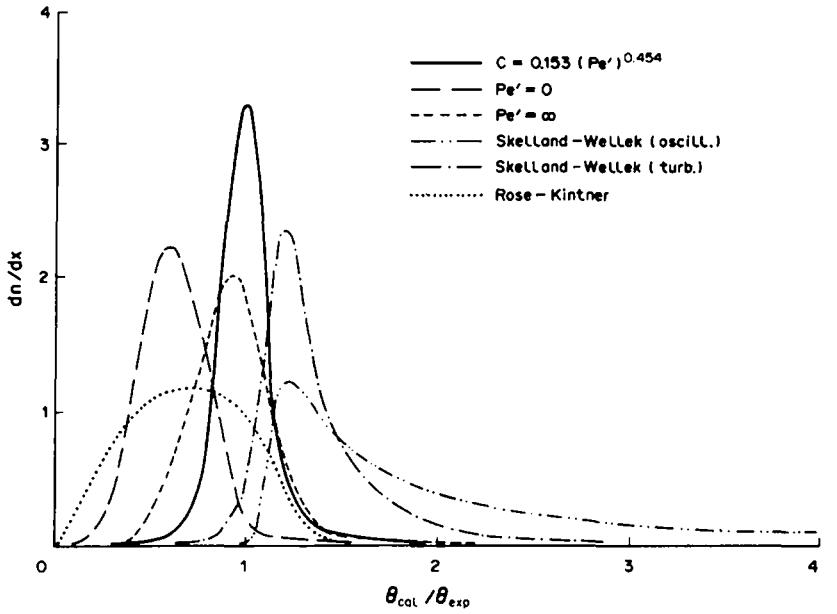

Figure 17. Probability density function of the predictions vs the ratio $\theta_{cal}/\theta_{exp}$.

The experiments are characterized by the continuous measurement of the average droplet temperature along the axis of the spray. They showed a high value of the condensation efficiency, much higher than that predicted by pure conduction and internal circulation models.

An empirical approach for the evaluation of the internal mixing inside the droplet is proposed as a function of the modified Peclet number. The comparison of the proposed method with the experimental data seems satisfactory.

Acknowledgements—The authors are grateful to N. Ciotti, who performed the experiments. Many thanks are due to A. Lattanzi for helpful assistance in the technical aspects of instrumentation and to Mrs B. Perra for typing the manuscript.

REFERENCES

BROWN, G. 1951 *Heat Transmission by Condensation of Steam on a Spray of Water Drops.* Institution of Mechanical Engineers, London.

CARRA, S. & MORBIDELLI, M. 1986 Transient mass transfer onto small particles and drops. In *Handbook of Heat and Mass Transfer*, Vol. 2 (Edited by CHEREMISINOFF, N. P.), pp. 59–109. Gulf, Houston, Tex.

CELATA, G. P., CUMO, M., FARELLO, G. E. & FOCARDI, G. 1987 Direct contact condensation of steam on a horizontal surface of water. *Wärme-u. Stoffübertrag.* **21,** 169–180.

CELATA, G. P., CUMO, M., FARELLO, G. E. & FOCARDI, G. 1989a A comprehensive analysis of direct contact condensation of saturated steam on subcooled liquid jets. *Int. J. Heat Mass Transfer* **32,** 639–654.

CELATA, G. P., CUMO, M., D'ANNIBALE, F., FARELLO, G. E. & FOCARDI, G. 1989b A theoretical and experimental study of direct contact condensation on water in turbulent flow. *Expl Heat Transfer* **2,** 153–172.

CELATA, G. P., CUMO, M., D'ANNIBALE, F. & FARELLO, G. E. 1989c Direct contact condensation of steam on droplets, ENEA Report NQDZ 1TS4B 89029.

CHUNG, J. N. & AYYASWAMY, P. S. 1977 The effect of internal circulation on the heat transfer of a nuclear reactor containment spray droplet. *Nucl. Technol.* **35,** 602–610.

CHUNG, J. N. & CHANG, T. H. 1984 A mathematical model of condensation heat and mass transfer to a moving droplet in its own vapor. *J. Heat Transfer* **106,** 417–424.

DHARMA RAO, V. & SARMA, P. K. 1985 Direct contact heat transfer in spherical geometry associated with phase transformation—a closed-form solution. *Int. J. Heat Mass Transfer* **28,** 1956–1958.

FORD, J. D. & LEKIC, A. 1973 Rate of growth of drops during condensation. *Int. J. Heat Mass Transfer* **16,** 61–64.

FORD, J. D. & LEKIC, A. 1980 Direct contact condensation of vapor on a spray of subcooled liquid droplets. *Int. J. Heat Mass Transfer* **23,** 1531–1537.

HADAMARD, J. S. 1911 Mouvement permanent lent d'une sphère liquide et visqueuse dans un liquide visqueux. *C. r. hebd. Séanc. Acad. Sci., Paris* **152,** 131.

HIJIKATA, K., MORI, Y. & KAWAGUCHI, S. 1984 Direct contact condensation of vapor of falling cooled droplets. *Int. J. Heat Mass Transfer* **27,** 1631–1640.

HUANG, L. J. & AYYASWAMY, P. S. 1987 Heat and mass transfer associated with a spray drop experiencing condensation: a fully transient analysis. *Int. J. Heat Mass Transfer* **30,** 881–891.

ISACHENKO, V. P. & SOLODOV, A. P. 1972 Heat transfer with steam condensation on continuous and on dispersed jets of liquid. *Teploenergetika* **19,** 35–39.

KÖNIG, G. & FROHN, A. 1983 Visualization of uniformly disintegrated liquid jets by a new observation technique. In *Proceedings Third International Symposium on Flow Visualization, Ann Arbor, Mich.* (Edited by JANG, W. J.), pp. 488–492.

KRONIG, R. & BRINK, J. C. 1950 On the theory of extraction from falling droplets. *Appl. scient. Res.* **A2,** 142.

LAMB, H. 1932 *Hydrodynamics*, 6th edn, p. 245. Cambridge Univ. Press, Cambs.

OHBA, K., KITADA, H. & NISHIGUCHI, A. 1982 Direct contact condensation on a high speed spray jet of subcooled water. In *Heat Transfer in Nuclear Reactor Safety* (Edited by BANKOFF, S. G. & AFGAN, N. H.). Hemisphere, Washington, D.C.

PASAMEHMETOGLU, K. O. & NELSON, R. A. 1987a Transient direct contact condensation on liquid droplets. Presented at the *ASME–ANS–AIChE National Heat Transfer Conf.*, Pittsburgh, Pa.

PASAMEHMETOGLU, K. O. & NELSON, R. A. 1987b Direct contact condensation on liquid droplets during rapid depressurization, Part 1: quasi-steady solution. Presented at the *ASME Winter A. Mtg*, Boston, Mass.

RAYLEIGH LORD, J. W. 1878 On the instability of jets. *Proc. Lond. math. Soc.* **10,** 4.

ROSE, P. M. & KINTNER, R. C. 1966 Mass transfer from large oscillating drops. *AIChE Jl* **12,** 530–534.

SCHNEIDER, J. M. & HENDRICKS, C. D. 1964 Source of uniform-size liquid droplets. *Rev. scient. Instrum.* **35,** 1349.

SKELLAND, A. H. P. & WELLEK, R. M. 1964 Resistance to mass transfer inside droplets. *AIChE Jl* **10,** 491–496.

WEINBERG, S. 1952 *Heat Transfer to Low Pressure Sprays of Water in a Steam Atmosphere.* Institution of Mechanical Engineers, London.

WIEGAND, H. 1970 On the break-up of a liquid jet in a sequence of uniform size liquid droplets. Technical translation of DVL-Report No. 608.